Event-triggered Consensus Control of Large-scale Inverter Air Conditioners for Demand Response

Jiatu Hong, *Student Member, IEEE,* Hongxun Hui, *Member, IEEE,* Hongcai Zhang, *Member, IEEE,*
Ningyi Dai, *Senior Member, IEEE,* and Yonghua Song, *Fellow, IEEE*

Abstract—The boom of fluctuating renewable energies puts forward higher requirements on reserve capacity for maintaining the power system balance. To address this issue, this letter investigates a novel distributed event-triggered consensus control (ETCC) method of large-scale inverter air conditioners (IACs) for demand response, which can achieve the same regulation objective and response speed while significantly relieving the communication burden compared with traditional time-scheduled consensus control methods. Based on Lyapunov stability theorem, we also prove the convergence of the ETCC with nonlinear protocol for massive IACs. Finally, the above models and methods are verified by numerical studies.

Index Terms—Demand response, inverter air conditioner, event-triggered consensus control, Lyapunov stability.

I. Introduction

POWER energy shortage puts forward a higher requirement on reserve capacity for maintaining the system balance. However, it may be difficult for traditional generating units (e.g., thermal power generators) to provide sufficient reserve capacity in the near future, because uncontrollable renewable energies are rapidly increasing to replace generating units. With the development of Internet of Things, demand response (DR) provided by massive distributed energy resources at demand side is regarded as a promising alternative solution. In this paper, inverter air conditioners (IACs) are particularly investigated due to: i) IACs have accounted for a major share in the market and occupied around 30% of the total social power consumption with significant regulation potential; ii) the power consumption of IACs can be flexibly controlled [1]; iii) IACs can be regulated temporarily while guaranteeing customers' comfort utilizing buildings' thermal inertia. In the projects in US [2] and China [3], customers with air conditioners can get control modules with functions of communication and control to participate in regulation services. The economic benefits are pretty attractive for both customers and power system operator.

Traditionally, IACs are aggregated and controlled for DR by the centralized framework, while it has a high requirement on the control center's computation performance and may threaten customers' data privacy [1]. By contrast, the distributed consensus control framework is more suitable for

regulating large-scale IACs due to advantages in privacy protection and lower communication infrastructure cost. However, traditional distributed time-scheduled consensus control (TSCC) methods feature periodic communication, which leads to waste of communication resources, especially facing large-scale controllable IACs [4].

To address this issue, this paper investigates the event-triggered consensus control (ETCC) of large-scale IACs for DR, which aims to improve the utilization efficiency of communication resources while achieving the same regulation objective and response speed as traditional TSCC methods.

II. Modeling of the IACs

The thermodynamic process of a room can be expressed as:

$$C_i \frac{dT_i(t)}{dt} = \frac{T_o(t) - T_i(t)}{R_i} - Q_i(t), \ \forall i \in \mathcal{I}, \ \forall t \in \mathcal{T}, \quad (1)$$

where C_i and R_i are the equivalent air heat capacity and thermal resistance of the i-th room, respectively; $T_i(t)$ and $T_o(t)$ are the i-th room's indoor temperature and the outdoor temperature at time t, respectively; $Q_i(t)$ is the cooling capacity of the i-th IAC at time t; $\mathcal{I}$ and $\mathcal{T}$ are sets of IACs and time slots, respectively.

The compressor accounts for the majority of one IAC's power consumption to generate cooling capacity. Based on the realistic test data, one IAC's operating power and cooling capacity can be simplified as linear with its compressor's operating frequency [1], which are expressed as:

$$P_i(t) = \kappa_{i1} f_i(t) + b_{i1}, \ \forall i \in \mathcal{I}, \ \forall t \in \mathcal{T}, \quad (2)$$

$$Q_i(t) = \kappa_{i2} f_i(t) + b_{i2}, \ \forall i \in \mathcal{I}, \ \forall t \in \mathcal{T}, \quad (3)$$

where $P_i(t)$ and $f_i(t)$ are the i-th IAC's operating power and compressor's operating frequency at time t, respectively. Symbols κ_{i1}, b_{i1}, κ_{i2} and b_{i2} are coefficients of the i-th IAC's operating power and cooling capacity, respectively. From (2)-(3), the IAC's electro-thermal conversion can be derived as:

$$Q_i(t) = \frac{\kappa_{i2}}{\kappa_{i1}} P_i(t) + \frac{\kappa_{i1} b_{i2} - \kappa_{i2} b_{i1}}{\kappa_{i1}}, \ \forall i \in \mathcal{I}, \ \forall t \in \mathcal{T}. \quad (4)$$

Equations (1)-(4) establish the relation between the real-time indoor temperature and the IAC's operating power. Therefore, we can regulate each IAC's power consumption to provide reserve capacity for the power system under guaranteeing each individual customer's comfortable indoor temperature. The total operating power of IACs is expressed as:

$$P_{\text{Total}}(t) = \sum_{i=1}^{N} P_i(t), \ \forall t \in \mathcal{T}, \quad (5)$$

where N is the total aggregated number of IACs.

(a) Aggregate IACs in the community for DR.

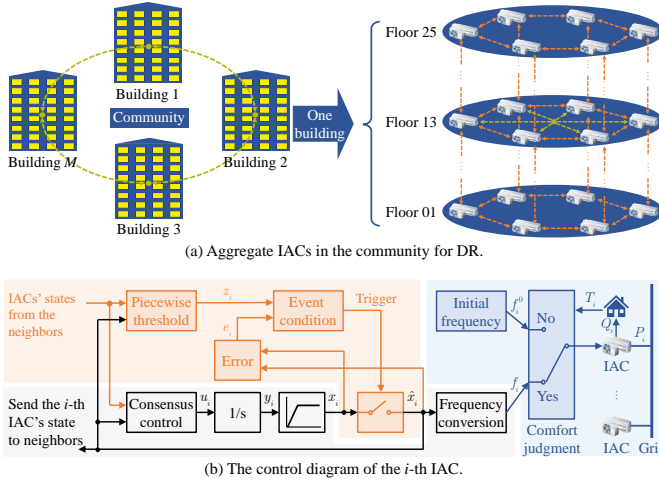(b) The control diagram of the i-th IAC.

Fig. 1. Event-triggered consensus control of IACs in the community for DR.

III. EVENT-TRIGGERED CONSENSUS CONTROL OF IACS

As shown in Fig. 1(a), IACs in the community are aggregated to provide reserve capacity for the power system. The proposed ETCC method is shown in Fig. 1(b), which mainly has three control objectives: i) Achieve the regulation requirement from the power system operator, including the required regulation capacity, response speed, and duration time; ii) Guarantee the desired comfortable indoor temperatures for all customers; iii) Improve the utilization efficiency of communication resources. Based on the proposed ETCC method, heterogeneous IACs can share the required regulation capacity according to their available regulation capacities.

A. Information Exchange Among IACs

The control diagram in Fig. 1(b) takes the i-th IAC as an example. Considering the IAC's power consumption is regulated by controlling the compressor's operating frequency, this paper defines the exchanged information (i.e., the state in ETCC) among IACs as follows:

$$\hat{x}_i(t) = \begin{cases} \dfrac{f_i(t) - f_i^0}{\overline{f_i} - f_i^0}, & \forall i \in \mathcal{I}, \forall t \in \mathcal{T}, \quad \text{Up regulation,} \\ \dfrac{f_i(t) - f_i^0}{\underline{f_i} - f_i^0}, & \forall i \in \mathcal{I}, \forall t \in \mathcal{T}, \quad \text{Down regulation,} \end{cases}$$
(6)

where $f_i(t)$ is the operating frequency of the i-th IAC's compressor at time t; f_i^0 is the compressor's initial operating frequency at the beginning of the regulation; $\underline{f_i}$ and $\overline{f_i}$ are the lower and upper limitations of the compressor's operating frequency, respectively. The state essentially indicates the normalized utilization ratio of the IAC's available capacity, ranging from 0 to 1. Therefore, the consensus of states means massive IACs utilize similar ratio of their heterogeneous available regulation capacities. Note that the rooms' physical parameters about thermodynamic models (e.g., C_i and R_i) do not need to be simulated in practical applications. The indoor temperature is an existing parameter and can be directly detected by temperature sensors. The variable that needs to be collected is the operating frequency of the IAC in (6), which can be measured locally by the controller.

Compared with the centralized control framework, IACs in the ETCC mainly communicate with their neighbors, which is conducive to reducing the communication infrastructure cost and control center's computation burden. Moreover, IACs only exchange the defined state $\hat{x}_i(t)$ with neighbors instead of uploading all the data to the control center. The exact physical parameters (e.g., f_i, f_i^0 and $\underline{f_i}$) are completely concealed to neighbors, which can enhance the privacy protection.

B. Design of Event-triggered Consensus Control

Compared with traditional TSCC methods, the communication and control in the ETCC are executed only when specific conditions are satisfied. The control event for the i-th IAC is triggered only when the error magnitude (i.e., the difference between the x_i and the latest event's state $\hat{x}_i$ in Fig. 1(b)) reaches a specific threshold. The error of the i-th IAC is defined as:

$$e_i(t) = x_i(t) - \hat{x}_i(t_{i,k}), \ t \in [t_{i,k}, t_{i,k+1}),$$
(7)

where $t_{i,k}$ is the k-th event instant of the i-th IAC. The threshold of the i-th IAC is defined as:

$$z_i(t) = \frac{\sigma_i}{4d_i} \sum_{j=1}^{N} a_{ij}[\hat{x}_j(t_{j,l}) - \hat{x}_i(t_{i,k})]^2, \ t \in [t_{i,k}, t_{i,k+1}),$$
(8)

where a_{ij} is the element of the adjacency matrix to indicate the communication network. For $a_{ij} = 1$, it means two relevant IACs are connected and thus information is exchanged between them during the regulation process. For $a_{ij} = 0$, the corresponding i-th IAC and j-th IAC are unconnected and not considered as neighbors. Symbol $t_{j,l}$ is the l-th event instant for the j-th IAC with $l = \arg \min_l \{t - t_{j,l} \mid t_{j,l} \leq t, \ l \in \mathbb{N}\}$; σ_i is the threshold coefficient for the i-th IAC; d_i is the number of neighbors for the i-th IAC. An event can be triggered for the i-th IAC if the following condition is satisfied:

$$e_i^2(t) \geq z_i(t).$$
(9)

If the condition in (9) is satisfied, the i-th IAC would communicate with its neighbors and the control protocol u_i can be updated:

$$u_i(t) = \sum_{j=1}^{N} a_{ij}[\hat{x}_j(t_{j,l}) - \hat{x}_i(t_{i,k})], \ t \in [t_{i,k}, t_{i,k+1}),$$
(10)

As shown in Fig. 1(b), based on the integral of $u_i(t)$, the intermediate variable y_i can be obtained. Then, the variable x_i is calculated as $x_i = sat(y_i) = \{y_i, \text{ when } 0 \leq y_i \leq 1; \ 1, \text{ when } y_i > 1; \ 0, \text{ when } y_i < 0\}$. In this way, $x_i(t) \in [0, 1]$ can be always maintained to guarantee that the IAC is adjusted in the available range. Finally, the defined state $\hat{x}_i(t)$ is set equal to the variable x_i when the control event is triggered. The regulation on compressor's operating frequency will be achieved by the conversion in (6). In addition, to guarantee the temperature comfort of customers, we design a comfort judgment block to recover the compressor's operating frequency back to the initial value f_i^0, if corresponding indoor temperature violates the customer's desired comfortable range.

To exclude the Zeno behavior, the key of the proof is to find a lower bound for any inter-event time $t_{i,k+1} - t_{i,k}$. At

the event instant $t_{i,k}$, $\hat{x}_i$ is updated as $\hat{x}_i(t_{i,k}) = x_i(t_{i,k})$, then $e_i(t_{i,k}) = 0$ is derived according to (7). For $t \in [t_{i,k}, t_{i,k+1})$, when the i-th IAC does not receive the information from its neighbor IACs, both $\hat{x}_i$ and $\hat{x}_j$ remain constant, and thus u_i remains constant according to (10). By integration, $y_i(t) - y_i(t_{i,k}) = (t - t_{i,k})u_i$ can be derived. The saturation function $x_i = sat(y_i)$ is monotonically increasing and the slope either equals to 1 or 0. Based on these characteristics, the following relation can be derived:

$$|y_i(t) - y_i(t_{i,k})| \geq |x_i(t) - x_i(t_{i,k})|. \quad (11)$$

At next event instant $t_{i,k+1}$, $e_i^2(t_{i,k+1}) = z_i(t_{i,k+1})$ holds:

$$|y_i(t_{i,k+1}) - y_i(t_{i,k})|^2 \geq |x_i(t_{i,k+1}) - x_i(t_{i,k})|^2 = e_i^2 = z_i. \quad (12)$$

Then, the following inequality can be derived as:

$$(t_{i,k+1} - t_{i,k})^2 \geq \frac{\sigma_i \sum_{j=1}^{N} a_{ij}(\hat{x}_j - \hat{x}_i)^2}{4d_i(\sum_{j=1}^{N} a_{ij}(\hat{x}_j - \hat{x}_i))^2}. \quad (13)$$

Based on Cauchy-Schwarz inequality, following inequality holds:

$$N \sum_{j=1}^{N} a_{ij}^2(\hat{x}_j - \hat{x}_i)^2 \geq (\sum_{j=1}^{N} a_{ij}(\hat{x}_j - \hat{x}_i))^2. \quad (14)$$

According to (13), (14) and the fact that $a_{ij} = a_{ij}^2$ (because $a_{ij} = 1$ or 0), the lower bound for any inter-event time can be derived as:

$$t_{i,k+1} - t_{i,k} \geq \frac{1}{2}\sqrt{\frac{\sigma_i}{d_i N}} > 0, \quad (15)$$

which completes the proof.

C. Convergence Analysis of the Proposed ETCC

To achieve the consensus of the outputs $\hat{x}$, a specific threshold should be designed for the ETCC with nonlinear protocol. The integral *Lyapunov* function [5] is utilized here and expressed as:

$$V = \sum_{i=1}^{N} \int_{\bar{y}}^{y_i}(sat(\omega) - \bar{y})d\omega, \quad \forall i \in \mathcal{I}, \quad (16)$$

where $\bar{y} = \sum_{i=1}^{N} y_i(0)/N$. From (16), $V \geq 0$ is obviously satisfied. The key is to prove $\dot{V} \leq 0$, as follows:

$$\begin{aligned}\dot{V} &= \sum_{i=1}^{N}(sat(y_i) - \bar{y})\dot{y}_i = \sum_{i=1}^{N}(x_i - \bar{y})\dot{y}_i \\ &= \sum_{i=1}^{N}\sum_{j=1}^{N} a_{ij}(e_i + \hat{x}_i)(\hat{x}_j - \hat{x}_i) \\ &\leq \sum_{i=1}^{N}(d_i e_i^2 - \frac{1}{4}\sum_{j=1}^{N} a_{ij}(\hat{x}_j - \hat{x}_i)^2).\end{aligned} \quad (17)$$

It can be seen that $\dot{V} \leq 0$ is satisfied if the threshold coefficient satisfies $\sigma_i \in (0, 1]$, $i \in \mathcal{I}$, i.e., consensus can be guaranteed.

Based on the above proposed ETCC algorithm and configured parameters with convergence, the final step is to design an overall communication framework for the buildings in the community. As shown in Fig. 1(a), one signal relay node is assigned for each building (i.e., the yellow node), which can communicate with neighbor buildings and nearby IACs (e.g.,

Parameters	Distributions	Parameters	Distributions
κ_{i1}	$\mathcal{U}(0.0285,0.0315)$ kW/Hz	R_i	$\mathcal{U}(1.9,2.1)$ °C/kW
b_{i1}	$\mathcal{U}(-0.42,-0.38)$ kW	C_i	$\mathcal{N}(390,78^2)$ kJ/°C
κ_{i2}	$\mathcal{U}(0.057,0.063)$ kW/Hz	T_i^{max}	$\mathcal{U}(27,28)$ °C
b_{i2}	$\mathcal{U}(-0.315,-0.285)$ kW	T_i^{set}	$\mathcal{U}(23,26)$ °C
f_i	$\mathcal{U}(15,30)$ Hz	T_o	32 °C

[1] $\mathcal{U}$ denotes uniform distributions, and $\mathcal{N}$ denotes normal distributions.
[2] T_i^{max} and T_i^{set} are customers' maximum allowable and set temperatures.

the IACs on floor 13). The relay nodes' state dynamics $\dot{r}_i$ are expressed as:

$$\dot{r}_i(t) = \sum_{j=1}^{N} a_{ij}(\hat{x}_j(t) - r_i(t)) + \lambda(P_{obj} - P_{DR}(t)), \quad (18)$$

where $P_{DR}(t)$ is the response capacity and can be calculated as $P_{DR}(t) = P_{Total}(0) - P_{Total}(t)$; P_{obj} is the required regulation capacity from the system operator; λ is the control coefficient. The first term, i.e., $\sum_{j=1}^{N} a_{ij}(\hat{x}_j(t) - r_i(t))$ indicates the information interaction between the relay node and its neighbor IACs. The second term, i.e., $\lambda(P_{obj} - P_{DR}(t))$ represents the proportional control component.

IV. CASE STUDIES

The effectiveness of the proposed ETCC to control IACs for DR is verified by a community with 20 buildings and 3000 IACs. The parameters of IACs, rooms' thermal characteristics and customers' comfort requirements are shown in Table I. It is assumed the system operator sends an up regulation signal to IACs at 14:30 PM. The requirement is 2 MW regulation capacity with 15 min duration time. The sampling period of controllers is set as 1 s. To compare the ETCC control effect, the threshold coefficient σ_i is set as 1 and 2 in two scenarios, respectively.

The control results of IACs are shown in Fig. 2. It can be seen from Fig. 2(a) that the regulation capacity of 2 MW is achieved in about 3 min, which is fast enough to provide operating reserve for the power system. The average temperature deviation at the end of the regulation process is about 1.7°C, which is within the allowable deviation range 2.0°C. Moreover, as shown in Fig. 2(b), states of IACs can achieve convergence in about 6 min. It means heterogeneous IACs can get similar regulation on their operation states to avoid significant impact on some specific users' comforts.

By contrast, the results in Figs. 2(c) and (d) are obtained under the $\sigma_i = 2$ scenario, which is beyond the proved convergence range in Section III-C. It can be seen that the operating power of IACs cannot be maintained steadily. There are even some power rises after the response time (i.e., 240~900s). More seriously, the states of IACs in Fig. 2 (d) occur significant oscillations, which may cause damages to IACs. The above two scenarios prove that the proposed parameter configuration method for ETCC can avoid oscillations to achieve a stable control effect for IACs.

Fig. 3 compares the performance of traditional TSCC and the proposed ETCC ($\sigma_i = 1$ scenario). Here the maximum value for σ_i (i.e., 1) is chosen in the derived convergence range $(0, 1]$, because a larger σ_i is intended to decrease the triggering
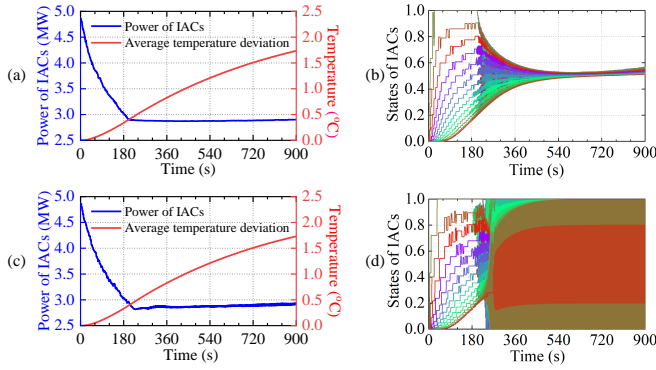
Fig. 2. The regulation process of IACs for DR based on ETCC. (a) The power of IACs and average temperature deviation with $\sigma_i = 1$; (b) State dynamics of IACs with $\sigma_i = 1$; (c) The power of IACs and average temperature deviation with $\sigma_i = 2$; (d) State dynamics of IACs with $\sigma_i = 2$.
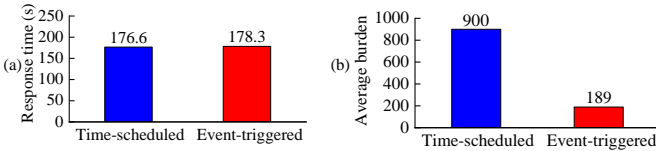

Fig. 3. Performance of TSCC and ETCC methods in terms of (a) Response time; (b) Average communication burden.

times. The communication period in TSCC is set as 1s. It can be seen from Fig. 3(a) that the response speeds are similar in two cases, i.e., 176.6s and 178.3s, respectively. However, in Fig. 3(b), the communication times are significantly decreased from 900 to 189 by ETCC. Hence, the proposed ETCC can improve the utilization efficiency of local communication resources by about fivefold.

The comparative case studies of the centralized control method [1] and other event-triggered control methods [6] are shown in Fig. 4. Both response speeds with the proposed ETCC method and the centralized control are adequate for meeting the requirement of providing reserve capacity (i.e., the response time should be less than 5 min [7]). Meanwhile, the proposed ETCC method has advantages in lower infrastructure cost, privacy protection and enhanced scalability, compared with the centralized control. When the threshold coefficient is set as 0.05, the comparative event-triggered control method cannot converge, as shown in Fig. 4(b). When the threshold coefficient is 0.02, the system converges, as shown in Fig. 4(c), (d). However, since the threshold coefficient is too small in this case, the benefit of the event-triggered control is lost. The average number of communication times is 884 for the comparative method, while it is only 189 using the proposed ETCC method.

The comparative case study with the sampling period of controllers as 2 s is shown in Fig. 5. It can be seen that if the sampling period is too large, the requirement of the response time (i.e., it should be less than 5 min [7]) for providing reserve capacity may not be satisfied.

V. CONCLUSION

This paper investigates the ETCC of large-scale IACs for DR. Compared with centralized control methods, the ETCC can reduce the control center's computation burden and enhance the privacy protection. Compared with traditional TSCC
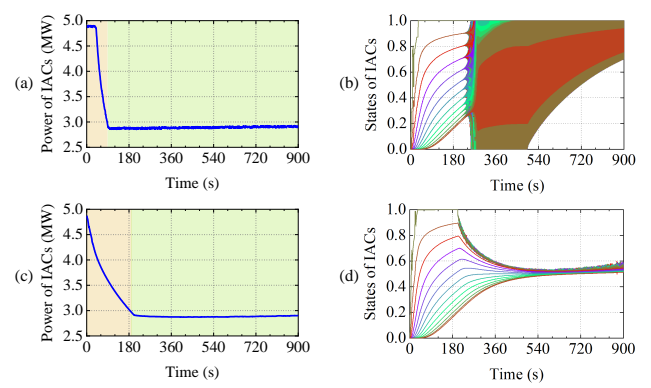

Fig. 4. Comparative case studies. (a) Power of IACs with the centralized control; (b) IAC states based on the comparative event-triggered control with threshold coefficient 0.05; (c) and (d) Power and states of IACs based on the comparative event-triggered control with threshold coefficient 0.02.
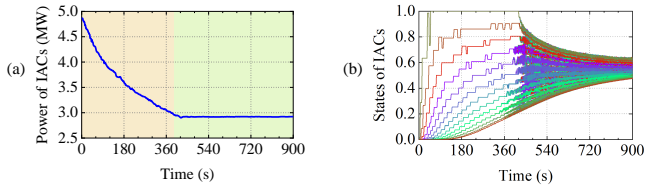

Fig. 5. The regulation process of IACs based on the ETCC with the sampling period as 2 s. (a) Power of IACs; (b) State dynamics of IACs.

methods, the proposed ETCC can achieve the same regulation objective and response speed while significantly relieving the communication burden. Moreover, a control parameter configuration method is designed utilizing *Lyapunov* theory to avoid state oscillations and achieve a stable control of IACs. The proposed approach can also be extended to other flexible resources, such as battery energy storage systems and water heaters. The ETCC can provide valuable reference for future smart grid with massive controllable loads based on the progressed Internet of Things technologies. The effectiveness of the proposed control method dealing with other application scenarios (e.g., the ancillary services with shorter time scale) needs to be further investigated.

REFERENCES

[1] M. Song, C. Gao, H. Yan, and J. Yang, "Thermal battery modeling of inverter air conditioning for demand response," *IEEE Trans. Smart Grid*, vol. 9, no. 6, pp. 5522–5534, Nov. 2018.

[2] Avangrid corporation, "UI demand response programs," Tech. Rep., 2016.

[3] H. Hui, Y. Ding, K. Luan, T. Chen, Y. Song, and S. Rahman, "Coupon-based demand response for consumers facing flat-rate retail pricing," *CSEE J. Power Energy Syst.*, Early Access, 2022.

[4] Y. Wang, Y. Tang, Y. Xu, and Y. Xu, "A distributed control scheme of thermostatically controlled loads for the building-microgrid community," *IEEE Trans. Sustain. Energy*, vol. 11, no. 1, pp. 350–360, Jan. 2020.

[5] W. Brogan, *Modern Control Theory*, 3rd ed. Pearson, 1990.

[6] G. Guo, L. Ding, and Q. Han, "A distributed event-triggered transmission strategy for sampled-data consensus of multi-agent systems," *Automatica*, vol. 50, no. 5, p. 1489–1496, May 2014.

[7] German transmission system operators, "Prequalification process for balancing service providers in Germany," Tech. Rep., 2020.